A PRELIMINARY BROAD-BAND SOURCE MODEL OF THE 2014 PAPANOA (Mw 7.3), MEXICO, EARTHQUAKE, USING THE EMPIRICAL GREEN'S FUNCTION TECHNIQUE

Jonatan ARREOLA-MANZANO* **Supervisor: Tomotaka IWATA****
MEE16701

ABSTRACT

In this study, a preliminary broadband source model for the 2014 Papanoa, Mexico, earthquake (M_w=7.3) was obtained through the empirical Green's function method. The waveforms of a small earthquake of magnitude M_w=5.1 which occurred in 2010, in the same region, and with a similar focal mechanism solution, were used to obtain synthetic time series for the mainshock. To estimate the simulation parameters *N* and *C*, source spectral ratios with broadband and strong motion data were used. Using those parameters, the position and the size of the SMGA were determined. The obtained source model is composed of one Strong Motion Generation Area (SMGA), with a size of 121 km^2. The obtained SMGA seems to correspond to one of the large slip area of the inversion models derived with teleseismic data. The relationship of the size of the SMGA and seismic moment of this event almost coincides to the empirical relationships obtained the previous study for the subduction earthquakes.

Keywords: subduction earthquake, the empirical Green's function method, the 2014 Papanoa, Mexico, earthquake, strong motion generation area.

1. INTRODUCTION

In the field of the strong-motion seismology, strong-ground motion is earthquake-induced ground motion capable of damaging a human-made environment (e.g. Panza et al., 2014). Strong ground motions are observed in the source areas of large earthquakes, i.e., near-source strong ground motions. Near-source strong ground motions are controlled by heterogeneous source rupture characteristics (e.g. Miyake et al., 2003; Asano and Iwata, 2012). Knowledge of the heterogeneity and rupture process of the earthquake source (that control the near source strong ground motions at the earthquake source) is essential for the improvement of seismic hazard assessment and both of critical tasks for the world scientific community and local governments.

The broadband source model is a model in terms of strong ground motion generation in the period range of several seconds down to 0.1 seconds. This period range corresponds to the natural vibration period of many buildings, bridges, and civil constructions. Estimation of the broadband source model is very important from the viewpoint of near-source strong ground motion generation. Moreover, comparison of the broadband source model with the slip model obtained from other seismic/geodetic data is useful for discussing the source characteristics and one of the key issues of seismic source modeling for future hypothetical earthquakes. In this paper, a preliminary broadband source model was obtained for the large subduction earthquake which occurred in Guerrero, Mexico (Mw 7.3) in 2014 using the empirical Green's function method.

*National Center for Disaster Prevention, Mexico.
**Professor, Disaster Prevention Research Institute, Kyoto University, Japan.

2. DATA

On April 18, 2014, at 09:27:25.50 a.m. local time (14:27:25.50 UTC), an M_w 7.3 earthquake struck the northwest portion of the Guerrero coast, Mexico. Its epicenter was calculated by the UNAM seismology group (2015) to be 17.375 N, 101.055 W at a depth of 15 km (Figure 1). In this study, we use the waveforms recorded by the engineering strong ground motion network of the National Autonomous University of Mexico, IINGEN-UNAM, the CENAPRED strong ground motion observation network, and by the permanent broadband/acceleration stations of the Mexican national seismic network, SSN-UNAM for earthquakes shown in Figure 2.

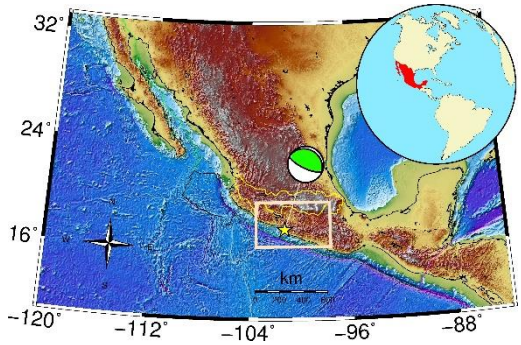

Figure 1. Study region.

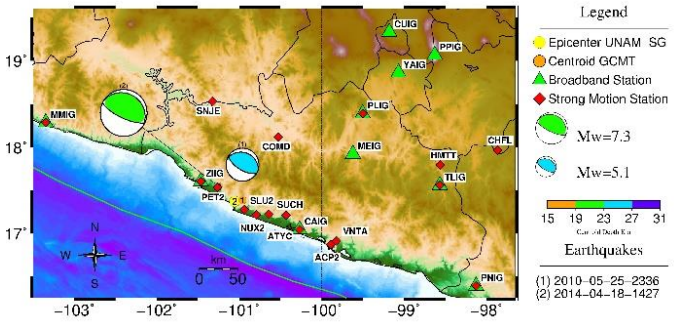

Figure 2. Detailed view of the study region.

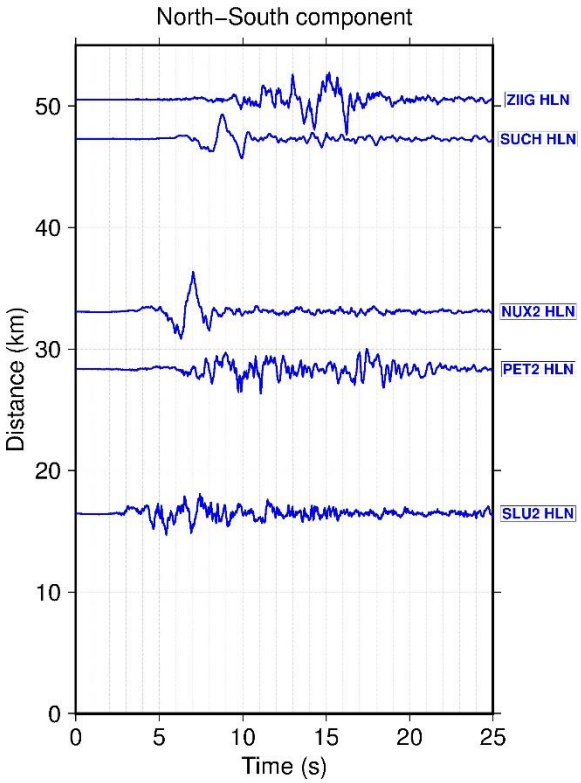

Figure 3. North-South component for the integrated velocity of the mainshock Papanoa earthquake for the five stations closest to the hypocenter.

Figure 1 shows the target area in this study with the GCMT solution of the 2014 Papanoa earthquake. Figure 2 is a small-scale map of the events and seismic station used in this study. Red diamonds indicate strong motion stations and green triangles indicate broadband stations. Figure 3 shows plotting of distance against time (for the mainshock) of the integrated North-South velocity waveforms, as the original ground motion data are acceleration records, for five stations within the 50 km of the epicentral distance. The waveforms recorded in the stations in the source region and to the west of the hypocenter (e.g. SLU2, PET2, ZIIG) show some complexity, whereas the waveforms recorded to the east (e.g. NUX2, SUCH) show a single clear S-wave packet. Amplitude and arrival time for the S-wave packet observed in stations to the west of the hypocenter suggest that the source for the strong motion generation is different than the source of strong motion generation for stations to the east.

3. METHODOLOGY

3.1. The Empirical Green's Function Method

In this study, the broad-band source model of the 2014 Papanoa earthquake was obtained by waveform modeling using the empirical Green's function method. Irikura (1986) proposes a methodology through which the observed seismic waveforms from appropriate small events *u(t)*, are used to reproduce the ground motion time series for large earthquakes *U(t)*. The synthetic time series for the main event are obtained through the superposition of the observed waveforms of small events convolved with a filter function *F(t)*. According to Irikura (1986) and Miyake et al. (2003), *U(t)* can be obtained through the following numerical equations,

$$U(t) = \sum_{i=1}^{N}\sum_{j=1}^{N}\frac{r}{r_{ij}}F(t) * [C \cdot u(t)], \quad (1)$$

$$t_{ij} = \frac{r_{ij}-r_0}{V_s} + \frac{\xi_{ij}}{V_r}, \quad (2)$$

$$F(t) = \delta\left(t - t_{ij}\right) + \frac{1}{n'^{(1-\frac{1}{e})}}\sum_{k=1}^{(N-1)n'}\left[\frac{1}{\frac{(k-1)}{e^{(N-1)n'}}}\delta\left\{t - t_{ij} - \frac{(k-1)T}{(N-1)n'}\right\}\right], \quad (3)$$

Eq. (1), *C* (real number) is the ratio of the stress drop between the target and element events, *N*, integer number, is the ratio of the fault dimensions between the large and small earthquakes. The distances from the observation point to the hypocenter of the small event and the subfault are *r* and r_{ij}, respectively. In Eq. (2), the delay time of the rupture from each subfault to the site of observation is t_{ij}, r_0 is the distance from the seismic station to the rupture starting point on the fault plane. The shear wave velocity of the propagation media is V_s, V_r is the speed of the rupture front. The variable ξ_{ij} represents the distance between hypocenter and each subfault, *n'* is an integer constant included to prevent the artificially periodicity. In Eq. (3), *F(t)* is a filter function which corrects the difference in the slip velocity-time function among large and small events, and *T* is the rise time for the large event (Miyake et. al., 2003). The scaling parameter *N* and *C* are derived by (Irikura, 1986; Miyake et al., 2003) as follows,

$$\frac{U_0}{u_0} = \frac{M_0}{m_0} = CN^3, \quad (4)$$

$$\frac{A_0}{a_0} = CN, \quad (5)$$

In Eq. (4), U_0 and u_0 indicate the constant level of the displacement spectra for the large and small events, respectively. M_0 and m_0 are the seismic moments of the target and element events, respectively. In Eq. (5), A_0 and a_0 indicate the flat levels of the acceleration spectra for the large and small events, respectively.

3.2. Spectral ratio for strong motion data

The observed source spectral S-wave spectral ratio for the strong motion data is expressed as,

$$\frac{S(f)}{s(f)} = \frac{O(f)}{o(f)} \cdot \frac{\frac{1}{r}e^{-\pi f r/Q_S(f)V_S}}{\frac{1}{R}e^{-\pi f R/Q_S(f)V_S}}, \quad (6)$$

where the propagation path effect is given by the geometrical spreading of the body waves and by a frequency-dependent attenuation factor *Q(f)* for the S-waves. *R* is the centroid distance of the large event and *r* is the centroid distance for the small event. The centroid distance was assumed to be the hypocentral distance for the small event.

3.3. Spectral ratio for broadband data

To obtain the reliable spectral ratios, we estimated them using the broadband station data. As S-wave portions of the mainshock in the broadband data are clipped at some stations, we used S-coda waves for the estimation. The observed S-coda wave spectral ratio is expressed as,

$$\frac{S(f)}{s(f)} = \frac{O(f)_{coda}}{o(f)_{coda}}, \tag{7}$$

where *O(f)* coda is the observed S-coda wave spectrum for the large event, and *o(f)* coda is the observed S-coda wave spectrum for the small event.

3.4. Amplitude spectrum

For obtaining the observed amplitude spectra, a time window of 40.96 seconds was used and applied a tapering of five percent window length applied, both for broadband and strong motion data. Regarding the strong motion data, the S-wave part was used to calculate the amplitude spectra from a starting time of two seconds before the S-wave onset (five percent of the time window, for tapering). For S-wave coda of the broadband data, the time window was taken from the two times of the S-wave lapse time plus the source time duration of the mainshock. We assumed the mainshock source duration is 20 seconds.

To obtain the observed amplitude spectrum the following formula was used:

$$O(f) = \sqrt{NS^2 + EW^2 + UD^2}, \tag{8}$$

where *NS* is the amplitude spectrum of the north-south component, *EW* is the amplitude spectrum of the east-west component, and *UD* is the amplitude spectrum of the up-down component.

4. RESULTS AND DISCUSSION

From the collected broadband (velocity) and strong motion (acceleration) records for the small and large events, source spectral ratios were obtained, and scaling parameters of *N* and *C* estimated. The *N* (integer number) parameter represents the ratio of fault dimension between target and element events. The *C* (real number) parameter represents the ratio of stress drop between large and small events. These two parameters can be obtained from the flat level of the longer and shorter period of the source amplitude spectral ratio (Miyake et al., 2003).

Figure 4 shows the observed source spectral ratios for broadband and strong motion stations (as seen in Figure 2). The average observed spectral ratio among nine broadband stations is shown in red solid line. The average spectral ratio among 17 strong motion stations is shown in blue line. Observed source spectral ratio for each broadband station is shown in brown dotted line, and observed source spectral ratio for each strong motion station is shown in light-blue lines. Using the flat levels values in the low frequency and high frequency range of the observed source spectral ratio and Eq. (4) and (5) it was possible to estimate the scaling parameters *N* and *C*. The *N*=5 and *C*=6.0 values were used to simulate the observed waveforms for stations shown in Figure 5.

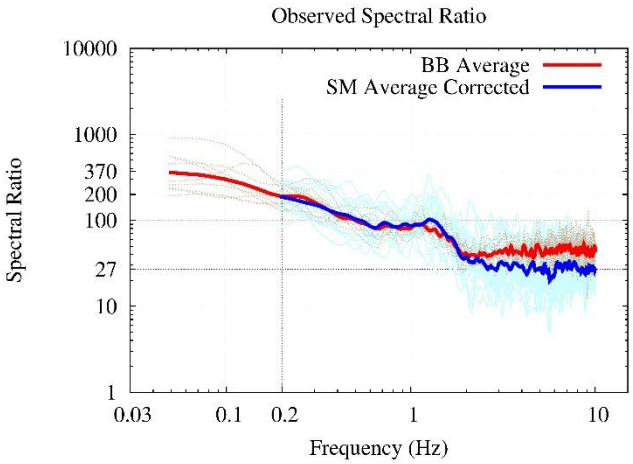

Figure 4. Observed source spectral ratios.

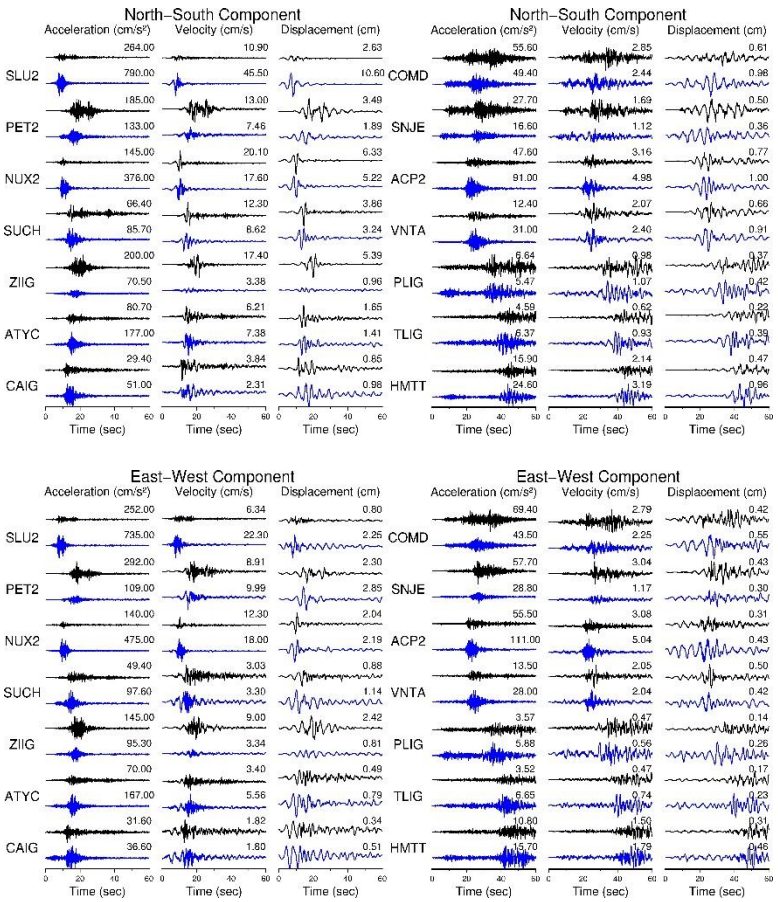

Figure 5. Comparison between the observed and synthetic acceleration, velocity and displacement waveforms. The upper black traces are observed, and the lower blue traces are synthetics waveforms. The waveforms are normalized by the maximum amplitude of the observed waveform. The numbers above the traces are the maximum amplitude of each trace.

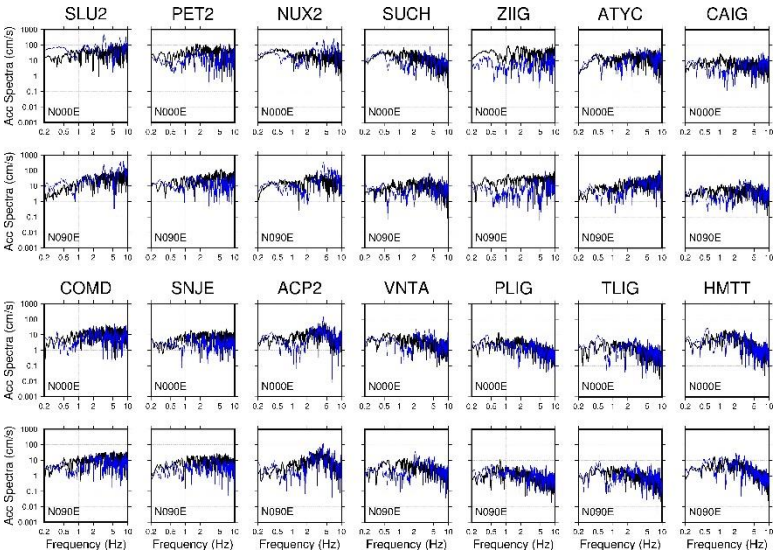

Figure 6. Comparison between the Fourier amplitude spectra of the observed (black) and synthetic accelerations (blue).

Parametric studies on the SMGA size, rupture starting point on the SMGA, and rise time were conducted. The values for the shear wave velocity, $\beta=3.5$ *km/s*, and the rupture velocity, $V_r=2.6$ *km/s* were fixed for these simulations. The quality of the agreement between the observed waveforms and synthetic ones was established by visual analysis, with reference to the correlation coefficient and residual term. The best simulation is one that gives correlation coefficients closest to 1.0 and residual terms closest to 0.0. Regarding stations to the east of the hypocenter (SLU2, NUX2, SUCH, ATYC, CAIG, ACP2, VNTA, PLIG, TLIG and HMTT), the comparison between observed and synthetic waveforms for displacement, velocity, and acceleration (N-S and E-W components showed good agreement as seen in Figure 5. Regarding sites to the west of the hypocenter (PET2, ZIIG, COMD and SNJE), except for PET2 and ZIIG, the waveforms comparison for displacement, velocity and acceleration for the horizontal components, showed acceptable agreements. Figure 6 shows the comparison between the observed and synthetic acceleration Fourier amplitude spectra at the same stations shown in Figure 5. Derived from the simulations, the length and width for the SMGA were about 11 km, respectively. Therefore, the size of the SMGA was estimated about 121 km^2 as seen in Figure 8.

5. CONCLUSIONS

In this study, a broad band source model for the 2014 Papanoa subduction earthquake was obtained using the empirical Green's function method

(EGFM). To obtain the simulation summation parameters *N* and *C*, for the EGFM, two different approaches were used to estimate the spectral source amplitude ratios. One approach was to obtain the observed spectral ratio from broadband data (S-coda wave spectral ratio) and the other was from strong motion data (S-wave spectral ratio). Both spectral ratios show similar characteristics with several scattering and gave the source model parameters. Simulated ground motions of the first pulse observed at stations to the east of the hypocenter synthesize observed data well. The preliminary SMGA model was obtained with a size of about 121 km^2. The obtained SMGA seems to correspond to one of the large slip area of the slip inversion result obtained with teleseismic data. Also, the obtained SMGA seems generally coincide to the empirical relationship between SMGA size and seismic moment derived by Iwata et al. (2013) for subduction earthquakes. On the contrary, there were poor agreements between observed and synthetic waveforms for the two closest stations to the west of the hypocenter. That would suggest that the obtained SMGA corresponds to the first SMGA and other SMGA is need to explain the observed waveforms in these two sites.

6. ACTION PLAN

In this paper, we attempted to obtain the broadband source model of the 2014 Papanoa, Mexico, earthquake using the empirical Green's function method. We succeeded to obtain the one SMGA model that reproduce well in the S-wave pulse, mainly observed in Eastern stations. We also found poor reproduction in the Western stations and suggested the existence of the second SMGA for the more reliable model. However, there are few stations that clearly observed the S-waves from the second SMGA and it is difficult to fix the rupture starting point and time of the second SMGA. We need to use more parametric study to find the source parameters of the second SMGA. After fixing this point, we can discuss the SMGA scaling, and the overall features of the 2014 Papanoa earthquake on the point of view of the broadband ground motion generation.

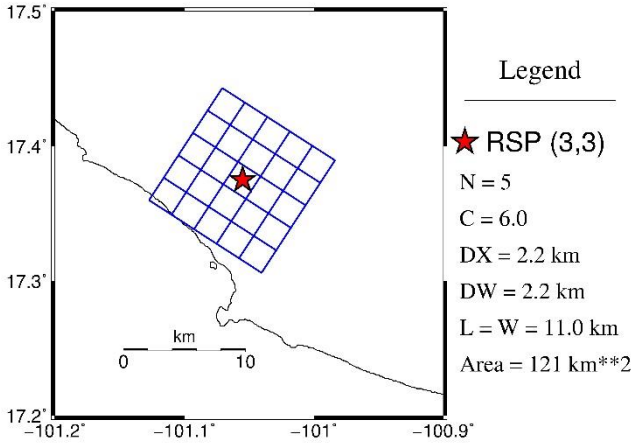

Figure 7. Strong motion generation area (SMGA) estimated by the empirical Green's function method for the 2014 Papanoa, Mexico, earthquake.

ACKNOWLEDGEMENTS

I would like to express my sincere gratitude to the supervisor Dr. Tomotaka IWATA, and advisors Dr. Bunichiro SHIBAZAKI and Dr. Toshiaki YOKOI for their continuous support, valuable suggestion and instruction during my study. Thanks are also due to Dr. Hiroe MIYAKE for providing the EGM program package to do the waveforms simulations.

REFERENCES

Asano, K., and Iwata, T., 2012, Earth Planets Space, 64, 1111-1123.
Irikura, K., 1986, in Proc. 7th Japan Earthquake Engineering Symp., 151-156, Tokyo, 10-12 Dec. 1986.
Iwata, T., Asano, K., and Kubo, H., 2013 Fall Meeting, Am. Geophys. Union, Abstract S43A-2470.
Miyake, H., Iwata, T., and Irikura, K., 2003, Bull. Seis. Soc. Am., 93, 2531-2545.
Panza, G. F., La Mura, C., Romanelli, F., and Vaccari F., 2014, Springer, New York, pp 252-260.
UNAM Seismology Group, 2015, Geofís. Int., 54-4, 363-386.